Available online at www.sciencedirect.com
SCIENCE DIRECT®
Catalysis Today 87 (2003) 205–212
CATALYSIS TODAY
www.elsevier.com/locate/cattod

Catalytic dehydrogenation of ethylbenzene with carbon dioxide: promotional effect of antimony in supported vanadium–antimony oxide catalyst

Min-Seok Park [a,b], Vladislav P. Vislovskiy [a], Jong-San Chang [a], Yong-Gun Shul [b], Jin S. Yoo [a], Sang-Eon Park [b,*]

[a] *Catalysis Center for Molecular Engineering, Korea Research Institute of Chemical Technology, P.O. Box 107, Yusong, Taejon 305-600, South Korea*
[b] *Department of Chemical Engineering of Yonsei University, Seodaemun-gu, Shinchon-dong 134, Seoul 120-749, South Korea*

Abstract

Alumina-supported vanadium oxide, VO_x/Al_2O_3, and binary vanadium–antimony oxides, $VSbO_x/Al_2O_3$, have been tested in the ethylbenzene dehydrogenation with carbon dioxide and characterized by S_{BET}, X-ray diffraction, X-ray photoelectron spectroscopy, hydrogen temperature-programmed reduction and CO_2 pulse methods. $VSbO_x/Al_2O_3$ exhibited enhanced catalytic activity and especially on-stream stability compared to VO_x/Al_2O_3 catalyst. Incorporation of antimony into VO_x/Al_2O_3 increased dispersion of active VO_x species, enhanced redox properties of the systems and formed a new mixed vanadium–antimony oxide phase in the most catalytically efficient $V_{0.43}Sb_{0.57}O_x/Al_2O_3$ system.

Keywords: Ethylbenzene; Dehydrogenation; Styrene; Carbon dioxide; Oxidant; Supported V–Sb oxide catalysts; Antimony promoter

1. Introduction

Styrene, an important monomer for synthetic polymers, is commercially produced by the vapor phase catalytic dehydrogenation of ethylbenzene (EBDH). This process is carried out at high-temperature (550–650 °C) with large excess of superheated steam. However, it is thermodynamically limited and energy consuming. Use of traditional oxidant—oxygen—allows to overcome the thermodynamic limitation, and, consequently, to operate at lower temperatures with an exothermic reaction. Combined EBDH process with the use of oxygen to oxidize hydrogen as a co-product and thus to displace the dehydrogenation equilibrium has been commercialized [1], but a process with direct use of oxygen for oxidative dehydrogenation has not been realized yet because of a significant loss of styrene selectivity by the production of carbon oxides and oxygenates [2]. Therefore, another desirable oxidant has sought for a long time.

Recently, several attempts were carried out to use carbon dioxide as an oxidant for EBDH and at the same time to utilize effectively CO_2, the global warming gas [3–26]. It has been reported that carbon dioxide could play a role as the soft oxidant as well as the diluent in the EBDH reaction with CO_2 (CO_2-EBDH), different from steam and oxygen employing as the diluent and the oxidant, respectively, in the non-oxidative and O_2-oxidative dehydrogenation [25]. Catalyst systems based on iron oxide, which is

* Corresponding author. Tel.: +82-42-860-7670; fax: +82-42-860-7676.
E-mail address: separk@pado.krict.re.kr (S.-E. Park).

0920-5861/$ – see front matter © 2003 Published by Elsevier B.V.
doi:10.1016/j.cattod.2003.10.015

known as an active component of industrial catalysts for non-oxidative EBDH process, were mainly used. Meanwhile, it is known that various V-containing oxide systems, such as V–Mg, V–Cr, V–P, V–Mo, V–Sb, etc. are active and selective in the relative reactions of selective oxidation, oxidative dehydrogenation and ammoxidation of lower paraffins and alkylaromatics [27–35], including the oxidative EBDH with oxygen [32–35]. However, V-containing catalysts for the CO_2-EBDH reaction have been reported only by few groups [13–16,23–26]. Suzuki and co-workers [13–15] reported that active carbon-supported vanadium catalysts exhibit high catalytic activity in EBDH to give styrene in the presence of carbon dioxide. However, it suffered from severe catalyst deactivation due to coke deposition. We also recently reported high selectivity (>95%) and catalytic activity of alumina-supported vanadium oxide (V/Al) in the CO_2-EBDH along with some arguments in favor of the carbon dioxide action as the soft oxidant [23–26]. Among a series of tested additives to VO_x/Al_2O_3 catalyst, antimony oxide was found to be the best second additional component improving the VO_x/Al_2O_3 catalyst activity and stability [26]. The objective of this work is to study the nature of promotional effect and role of antimony on the improved $VSbO_x/Al_2O_3$ catalyst in the CO_2-EBDH reaction.

2. Experimental

V/Al and VSb/Al catalysts were prepared by impregnation of activated alumina (Aldrich 19,996-6, $S_{BET} = 121\,m^2/g$) with aqueous solutions of ammonium metavanadate and antimony (III) chloride (Aldrich) along with tartaric acid. Subscript numbers of V and Sb in the formulae of $VSbO_x/Al_2O_3$ indicate the atomic percentages of the element in the supported binary system. The impregnated samples were dried at 120 °C and then calcined in air at 600 °C for 4 h. The total amount of the supported oxide component was 20 wt.%.

The calcined samples were characterized by means of BET specific surface area (SSA) measurements, X-ray diffraction (XRD), X-ray photoelectron spectroscopy (XPS), hydrogen temperature-programmed reduction (H_2-TPR), and CO_2 pulse method. SSA data were calculated from N_2 adsorption isotherms using a Micrometrics model ASAP 2400. XRD patterns were recorded on a Rigaku D/MAX-3B diffractometer using monochromatic Cu Kα radiation. The X-ray photoelectron spectra were obtained using an ESCALAB MK II spectrometer provided with a hemispherical electron analyzer and Al anode X-ray exciting source (Al Kα = 1487.6 eV). The binding energies (BE) were referred to the adventitious C 1s peak at 284.6 eV. For the Sb 3d core level spectra, the less intense Sb $3d_{3/2}$ peak of the Sb 3d doublet was taken for calculation based on the overlapping of the principal Sb $3d_{5/2}$ peak with the much more intense O1s peak. V $2p_{3/2}$ peak fitting was performed using symmetrical Gaussian–Lorenzian (80/20) lines with the following constraints for all oxidation states: non-linear Shirley background subtraction, an intensity ratio of V $2p_{3/2}$ to V $2p_{1/2}$ of 2.19, and a doublet separation (V $2p_{1/2}$–V $2p_{3/2}$) of 7.3–7.6 eV. Temperature-programmed reduction of the catalysts with hydrogen (5 vol.% H_2 in helium) was performed from 100 to 900 °C with heating rate of 10 °C/min in a conventional flow system equipped with a TCD detector for monitoring of the H_2 consumption. The samples (100 mg) were previously calcined in a flow of air at 600 °C for 1 h and then cooled down to 100 °C. In order to estimate the re-oxidizability with carbon dioxide of the pre-reduced catalysts, CO_2 pulse experiments were conducted at 600 °C in the quartz reactor with 200 mg of the catalyst. Prior to these experiments, the catalysts were partially reduced at 600 °C for 30 min in 5 vol.% H_2 in He flow. Pulses of carbon dioxide (250 μl CO_2) were injected into inert helium flow (30 cm^3/min) using gas sampling valve installed between the sample inlet and GC column.

The catalytic tests in the CO_2-EBDH reaction were carried out in a micro-activity test unit (Zeton, MAT 2000) with a fixed bed isothermal reactor under atmospheric pressure. A catalyst sample of 1 g was placed into reactor on a quartz wool support. Ethylbenzene was introduced by a syringe pump with a feed 8.2 mmol/h and supplied into the reactor with a carrier gas mixture CO_2 and N_2 (total flow rate: 45 cm^3/min). Nitrogen was used as inert diluent component as well as the internal standard for gas analysis. Gas components of the reaction mixture (H_2, N_2, CO, CH_4, CO_2) were analyzed by the TCD of the on-line gas chromatograph. Liquid products (benzene, toluene, ethylbenzene, styrene) were collected each 30 min

and analyzed by FID of the GC. Catalyst behavior was characterized by EB conversion degree, X(EB), initial yield of styrene after 1 h on-stream, Y_1, selectivity to styrene, S(ST), and relative loss of styrene yield after 4 h time-on-stream, $\mathrm{RLSY}(4) = Y_1 - Y_4/Y_1$.

3. Results

Table 1 summarizes the catalytic behaviors of alumina-supported vanadium oxide and V–Sb oxide catalysts in the CO_2-EBDH reaction at 595 °C. For this reaction, styrene is a main product. Only small amounts of benzene and toluene are obtained as by-products in the condensate along with traces of methane in gaseous products. All catalysts studied demonstrate high selectivity to styrene (>95%). The V/Al catalyst exhibits initially high styrene yield ($Y_1 \sim 71\%$). As the reaction proceeds, catalytic activity decreases significantly. This was mainly due to coke formation, as evidenced by intense CO_x-evolution to give the recovered activity during the reoxidation of the used catalyst in an air stream at more than 550 °C; over-reduction of vanadium oxidation state also takes place. The addition of antimony oxide, which is almost inactive by itself [26], into V/Al increases not only the initial styrene yield (up to $Y_1 = 76\%$), but also provides stable catalytic performance. Among the VSb/Al systems, the $V_{0.43}Sb_{0.57}$/Al catalyst is found to be the best one.

The XRD patterns of fresh and used V/Al and VSb/Al catalysts are shown in Fig. 1. Besides the weak diffraction lines of Al_2O_3, the distinct reflections of the V_2O_5-phase, shcherbinaite (41–1426 file in the JCPDS database), are observed in the fresh V/Al. After catalytic testing, V_2O_5-type phase transforms into V_2O_3, karelianite (34–0187). On the other hand, the fresh VSb/Al catalysts do not contain crystalline V_2O_5-type phases, but the XRD pattern of the fresh $V_{0.43}Sb_{0.57}$/Al points to the presence of a mixed vanadium–antimony oxide phase, which is assignable to $V_{1.1}Sb_{0.9}O_4$ by the appearance of the most intensive peak $2\Theta = 26.687°$ (47–1496 file in the JCPDS database). This phase remains in the used catalyst.

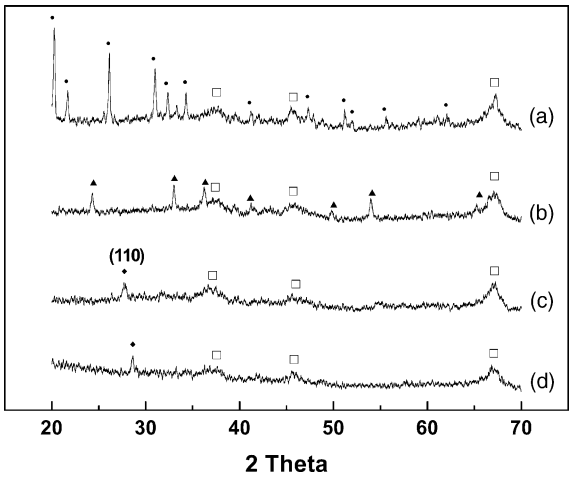

Fig. 1. XRD patterns of (a, c) fresh and (b, d) used samples of (a, b) V/Al and (c, d) $V_{0.43}Sb_{0.57}$/Al catalysts. (●) V_2O_5 (shcherbinaite); (▲) V_2O_3 (karelianite); (◆) $V_{1.1}Sb_{0.9}O_4$; (□) Al_2O_3.

Table 2 summarizes the spectral parameters of V and Sb components and results of deconvolution of V $2p_{3/2}$ peak taken from XP spectra of the V/Al and VSb/Al catalysts after the CO_2-EBDH reaction. The BEs of V $2p_{3/2}$ (517.2–517.6 eV) for the fresh V/Al and VSb/Al catalysts are corresponded to V^{5+} species [36,37]; the incorporation of antimony into V/Al increases the BE (and the oxidation state) of surface vanadium species. All VSb/Al catalysts show almost the same BEs for Sb $3d_{3/2}$, identifying as the

Table 1
Catalytic behavior of the V/Al and VSb/Al oxides in the CO_2-EBDH[a]

Catalyst	SSA (m^2/g)		After 1 h on-stream			RLSY(4) (%)
	Fresh	Used	X(EB) (%)	Y(ST) (%)	S(ST) (%)	
V/Al	78	65	74.8	70.7	94.5	21.3
$V_{0.87}Sb_{0.13}$/Al	74	62	79.8	75.8	95.0	11.6
$V_{0.43}Sb_{0.57}$/Al	87	88	79.9	76.0	95.1	3.3
$V_{0.25}Sb_{0.75}$/Al	104	109	73.9	71.2	96.3	6.7

[a] X(EB), ethylbenzene conversion; Y(ST), styrene yield; S(ST), styrene selectivity; RLSY(4), loss of styrene yield after 4 h on-stream relative to that after 1 h on-stream. Reaction conditions: $T = 595$ °C. $EB/CO_2 = 1$ (molar ratio).

Table 2
XPS analysis of V/Al and VSb/Al oxide catalysts and results of deconvolution of V $2p_{3/2}$ peaks of the catalysts used in the CO_2-EBDH[a]

Sample	V $2p_{3/2}$		Sb $3d_{3/2}$		V^{5+}			V^{4+}			V^{3+}		
	BE	FWHM	BE	FWHM	BE	FWHM	%	BE	FWHM	%	BE	FWHM	%
V/Al (F)	517.2	1.90											
V/Al (U)	517.1	3.16			517.5	2.27	49.5	516.0	2.26	33.7	515.0	2.53	16.8
$V_{0.87}Sb_{0.13}$/Al (F)	517.4	2.19	540.3	2.14									
$V_{0.87}Sb_{0.13}$/Al (U)	517.1	2.96	540.2	2.03	517.4	2.80	61.0	516.0	2.80	30.5	515.0	2.80	8.5
$V_{0.43}Sb_{0.57}$/Al (F)	517.6	2.18	540.2	2.34									
$V_{0.43}Sb_{0.57}$/Al (U)	517.7	2.34	540.2	2.07	517.8	2.80	83.9	516.0	2.80	16.1	–	–	–

[a] BE, binding energy (eV); FWHM, full width at half maximum (eV); F, fresh; U, used.

Sb^{5+} species [36]. Parameters of the Sb 3d peaks for these samples remain unchanged after catalytic runs. BEs of V $2p_{3/2}$ peaks for the VSb/Al catalysts remain almost unchanged after catalytic measurement, but full width at half maximum (FWHM) of the V $2p_{3/2}$ for the used V/Al catalyst is significantly increased relative to the fresh one, i.e., from 1.90 to 3.16 eV, revealing the notable reduction of surface vanadium species during the reaction. To interpret the change of FWHM of the V $2p_{3/2}$ peaks after reaction, they were fitted for V^{5+}, V^{4+} and V^{3+} components using the same method performed by the previous work [30]. The results of deconvolution point out that the incorporation of antimony into the V/Al catalyst increases the content of V^{5+} species very much as compared to that of the V/Al catalyst and, moreover, the used $V_{0.43}Sb_{0.57}$/Al catalyst practically does not contain V^{3+} species as the deeply reduced oxidation state.

H_2-TPR profiles of the V/Al and $V_{0.43}Sb_{0.57}$/Al catalysts are presented in Fig. 2. The reduction pattern of V/Al sample comprises three peaks, i.e., two intense and sharp high-temperature peaks centered at 663 and 783 °C and a low-temperature peak centered at 500 °C. The high-temperature peaks are similar to those detected in the literature [38–40], which are attributed to the reduction of bulk vanadium pentoxide to V_6O_{13} at 663 °C and to V_2O_4 at 783 °C. The low-temperature peak is analogous to the one that was assigned to the reduction of supported V_2O_5-phase in the VO_x/α-Al_2O_3 system [41]. Judging from the

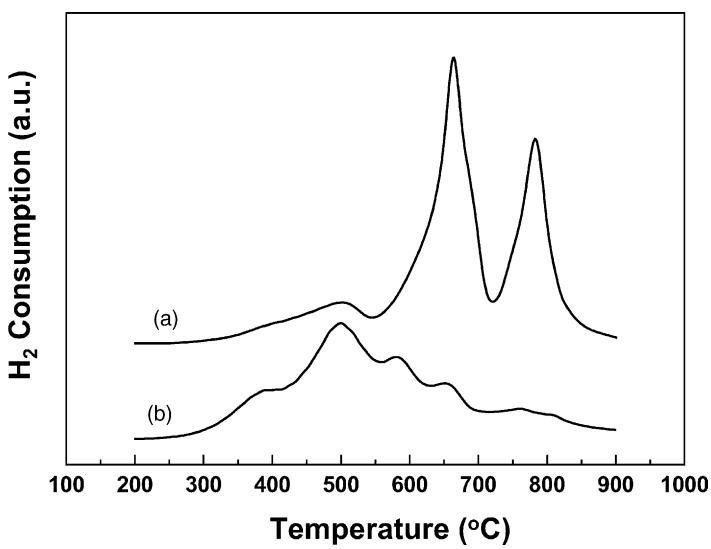

Fig. 2. H_2-TPR profiles of (a) V/Al and (b) $V_{0.43}Sb_{0.57}$/Al catalysts.

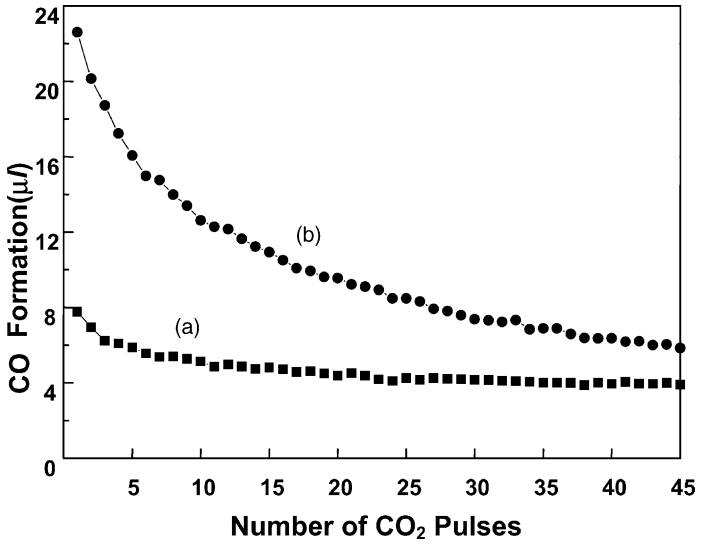

Fig. 3. Amounts of CO formed under pulse injections of CO_2 on pre-reduced (a) V/Al and (b) $V_{0.43}Sb_{0.57}$/Al oxide catalysts at 600 °C (see text for test conditions).

result, it is reasonable that the high-temperature peaks correspond to the reduction of three-dimensional V_2O_5, whereas the low-temperature peak corresponds to the surface vanadium oxide dispersed on the support. For the H_2-TPR profile of the $V_{0.43}Sb_{0.57}$/Al catalyst, the highest-temperature peak at 783 °C disappears completely and the intensity of the second one centered at 655 °C decreases greatly. Instead, the low-temperature peak becomes the dominant one. The broadening of this peak implies a higher heterogeneity and reducibility of vanadium species. These H_2-TPR data clearly reveal that incorporation of the antimony promoter into V/Al increases the reducibility of surface vanadium oxide and the amount of mobile oxygen species.

The amounts of CO produced according to sequential injections of CO_2 pulses at 600 °C onto the pre-reduced catalysts are plotted in Fig. 3. The reactivity of the catalysts for the CO_2 pulse reaction reflects the re-oxidizability of the reduced surfaces. The formation of CO over the $V_{0.43}Sb_{0.57}$/Al catalyst is notably large during the first several CO_2 pulses compared with that over the V/Al catalyst, implying that the partially reduced $V_{0.43}Sb_{0.57}$/Al catalyst is much easily interacted with CO_2 compared with the partially reduced V/Al catalyst. Moreover, when the total amount of CO produced up to 45 CO_2 pulses is estimated on the basis of the content of V_2O_5 in the catalysts, the data clearly point out the much high re-oxidizability of the $V_{0.43}Sb_{0.57}$/Al catalyst, i.e., 0.268 mol CO/mol V_2O_5 for $V_{0.43}Sb_{0.57}$/Al vs. 0.041 mol CO/mol V_2O_5 for V/Al.

4. Discussion

Catalytic results of Table 1 reveal that the catalytic activity is mainly determined by supported vanadium oxide species while the catalyst stability is controlled by antimony oxide. Although the initial styrene yields over Al_2O_3-supported V–Sb oxide catalysts containing a medium level of Sb-content are slightly higher, their activities do not differ substantially when they are compared among themselves and with VO_x/Al_2O_3. However, the catalyst stability is much improved by the addition of the antimony promoter and its stability is much dependent on the V/Sb ratio in the catalysts. Among the supported V–Sb oxide catalysts, $V_{0.43}Sb_{0.57}O_x/Al_2O_3$ is the most active and stable one.

XRD data shows the difference between the dispersion of the supported VO_x-component in the V/Al and VSb/Al catalysts. The fresh V/Al sample contains crystalline V_2O_5-phase, but this phase is transformed into V_2O_3 phase during the reaction. However, active

VO_x-component in the fresh and used VSb/Al catalysts is amorphous. The VO_x species was consistently observed only in a $V_{0.9}Sb_{0.1}O_x/Al_2O_3$ system with high V-concentration by means of laser Raman spectroscopy [42], which is very sensitive to the presence of VO_x species [43]. Raman spectra (not presented here) of the fresh sample showed a high background and only the bands corresponding to V_2O_5-phase with very low intensity [42]. However, after the catalytic test, no such a band was detected in the spectrum of the used sample, implying that the VO_x-phase looses its crystallinity and the oxide becomes spread on the surface as amorphous vanadium oxides. Therefore, it is concluded that VO_x active component of the VSb/Al catalysts is well dispersed on the support surface different from the V/Al catalyst.

Catalytic behavior for selective oxidation on vanadium oxide-based catalysts is related with the redox properties of vanadium species [28,29,44–46]. It is generally accepted that active sites for these systems are to be the surface vanadium cations operating according to a Mars–van-Krevelen redox mechanism. It can consequently be suggested that the easier redox cycle is an important factor to design the more effective catalyst [35]. The results of the study of oxidative dehydrogenation of lower paraffins over VO_x/Al_2O_3 and $V_{0.9}Sb_{0.1}O_x/Al_2O_3$ catalysts by differential scanning calorimetry show that reaction occurs via a stepwise redox mechanism with the participation of lattice oxygen from the catalyst [47]. When the supported VO_x-component is modified with antimony, the amount of reactive oxygen is increased and reduction–reoxidation cycles of vanadium ion proceed more efficiently. At the same time, the addition of antimony decreases the rate of coke formation [30,47,48], which explains the observed improvement in catalytic stability.

There is no doubt about redox nature of catalytic action of our V/Al and VSb/Al catalysts in the CO_2-EBDH reaction. The surface and even the bulk of unstable V/Al catalyst are reduced strongly under reaction conditions: V_2O_5-type phase transforms into V_2O_3, and the latter is able to be reoxidized to V_2O_5 in a flow of air restoring its yellow color and initial activity. It is worthwhile to note that V_2O_3 was the only vanadium species observed in XRD patterns of both fresh and used samples of vanadium oxide/active carbon catalyst, which showed very low stability in the CO_2-EBDH [13]. Deep vanadium reduction extent from V^{5+} to V^{3+} also seems to be one of the main reasons of the deactivation of our V/Al catalyst because the reoxidation of these strongly reduced active sites can become the rate-limiting step. This was confirmed by pulse and DSC techniques for the V_2O_5/Al_2O_3 catalyst for oxydehydrogenation of ethane [49]. In propane ammoxidation on V–Sb oxide catalysts, Centi et al. [50,51] also reported the relatively low re-oxidizability of the reduced supra-surface vanadium oxide species which is responsible for the unselective conversion of propane to carbon oxides, forming usually from strongly adsorbed organic intermediates similar to coke precursors. Datka et al. [52] suggested that carboxylate species are formed as coke precursor in carbon oxides atmosphere on alumina surface. Taking into account the fact that EB is much stronger reductant than ethane or propane [45], adsorption of EB on the non-properly regenerated active sites could hamper the redox cycle and become the reason of decreasing of activity of the V/Al catalyst. The observed enhancement of the catalytic behavior as a result of the addition of antimony oxide seems to be related with the improved catalyst reducibility (H_2-TPR of Fig. 2) and re-oxidizability by CO_2 (Fig. 3).

The role of antimony in the Sb-poor $VSbO_x/Al_2O_3$ catalysts could be interpreted as a ‘spillover oxygen donor’ in the frame of the ‘remote control mechanism’ theory elaborated by Delmon [53]. A key to maximize catalytic performance of active reducible oxides, such as MoO_3 [54,55] or V_2O_5 on alumina in the present work is to stabilize oxide surfaces at high or only slightly reduced suboxide oxidation state allowing the reduction–oxidation cycles of catalytic surfaces to proceed rapidly and smoothly. Addition of ‘spillover oxygen donor’ phases, like antimony oxide, to the reducible oxides (‘spillover oxygen acceptor’) contributes to inhibition of their deep reduction, which may be attributable to the capability of spillover oxygen species to reoxidize the reduced active sites with high efficiency [54,55]. And it could suppress the formation of polymeric residues, which are hard to remove and often become precursors to complete oxidation products [55] and coke [47,48]. The formation of active oxygen species with the similar nature could occur during the dissociative adsorption of CO_2 [56]. The better dispersion of vanadium oxide component

on the support surface also contributed to the better stability of the VSb/Al catalysts providing easier reducible spread active VO_x-component with increased amounts of mobile lattice oxygen. The most stable $V_{0.43}Sb_{0.57}$/Al catalyst with the XRD-detectable $V_{1.1}Sb_{0.9}O_4$ phase practically does not contain after catalytic test (XPS data) deeply reduced vanadium ion, V^{3+}. This is consistent with the fast reoxidation of the similar reduced vanadium antimonate phase [51].

5. Conclusions

Antimony oxide was found to be an effective co-component of alumina-supported vanadium oxide catalysts for the CO_2-EBDH reaction improving its activity and especially on-stream stability. Incorporation of antimony into VO_x/Al_2O_3 increases dispersion of the active VO_x-component, enhances redox properties of the systems and forms a new mixed V–Sb oxide phase $V_{1.1}Sb_{0.9}O_4$ in the most efficient binary $V_{0.43}Sb_{0.57}O_x/Al_2O_3$ catalyst.

Acknowledgements

This work was performed for the Greenhouse Gas Research Center, one of the Critical Technology-21 Programs, funded by the Ministry of Science and Technology of Korea (MOST). VPV thanks the MOST for the visiting scientist fellowship. We thank Daebo Industries Co. (Korea) for financial support.

References

[1] M.M. Bhasin, J.H. McCain, B.V. Vora, T. Imai, P.R. Pujado, Appl. Catal. A 221 (2001) 397.
[2] F. Cavani, F. Trifirò, Appl. Catal. A 133 (1995) 219.
[3] T. Inui, M. Anpo, K. Izui, S. Yanagida, T. Yamaguchi (Eds.), Advances in Chemical Conversions for Mitigating Carbon Dioxide, Stud. Surf. Sci. Catal. 114 (1998).
[4] M. Sugino, H. Shimada, T. Turuda, H. Miura, N. Ikenaga, T. Suzuki, Appl. Catal. A 121 (1995) 125.
[5] J.S. Yoo, Catal. Today 41 (1998) 409.
[6] N. Mimura, I. Takahara, M. Saito, T. Hattori, K. Ohkuma, M. Ando, Stud. Surf. Sci. Catal. 114 (1998) 511.
[7] N. Mimura, I. Takahara, M. Saito, T. Hattori, K. Ohkuma, M. Ando, Catal. Today 45 (1998) 61.
[8] N. Mimura, M. Saito, Catal. Lett. 58 (1999) 59.
[9] N. Mimura, M. Saito, Appl. Organometal. Chem. 14 (2000) 773.
[10] N. Mimura, M. Saito, Catal. Today 55 (2000) 173.
[11] M. Saito, H. Kimura, N. Mimura, J. Wu, K. Murata, Appl. Catal. A 239 (2003) 71.
[12] T. Badstube, H. Papp, R. Dziembaj, P. Kustrowski, Appl. Catal. A 204 (2000) 153.
[13] Y. Sakurai, T. Suzaki, N. Ikenaga, T. Suzuki, Appl. Catal. A 192 (2000) 281.
[14] N. Ikenaga, T. Tsuruda, K. Senma, T. Yamaguchi, Y. Sakurai, T. Suzuki, Ind. Eng. Chem. Res. 39 (2000) 1228.
[15] Y. Sakurai, T. Suzaki, K. Nakagawa, N. Ikenaga, H. Aota, T. Suzuki, J. Catal. 209 (2002) 16.
[16] A. Sun, Z. Qin, J. Wang, Appl. Catal. A 234 (2002) 179.
[17] J.-S. Chang, S.-E. Park, M.-S. Park, Chem. Lett. (1997) 1123.
[18] J.-S. Chang, S.-E. Park, W.Y. Kim, M. Anpo, H. Yamashita, Stud. Surf. Sci. Catal. 114 (1998) 387.
[19] J. Noh, J.-S. Chang, J.-N. Park, K.Y. Lee, S.-E. Park, Appl. Organometal. Chem. 14 (2000) 815.
[20] J.-N. Park, J. Noh, J.-S. Chang, S.-E. Park, Catal. Lett. 65 (2000) 75.
[21] S.-E. Park, J.-S. Chang, Y.K. Park, M.-S. Park, C.W. Lee, J. Noh, US Patent 6 037 511 (2000).
[22] S.-E. Park, J.S. Yoo, J.-S. Chang, K.Y. Lee, M.-S. Park, Preprints Am. Chem. Soc., Fuel Chem. Div. 46 (1) (2001) 115.
[23] S.-E. Park, J.-S. Chang, V.P. Vislovskiy, M.-S. Park, K.Y. Lee, J.S. Yoo, Proceedings of the Sixth International Conference on Carbon Dioxide Utilization, Breckenridge, CO, USA, September 2001, Book of Abstracts, p. 96.
[24] J.-S. Chang, M.-S. Park, V.P. Vislovskiy, S.-E. Park, J.S. Yoo, Preprints Am. Chem. Soc., Fuel Chem. Div. 47 (2002) 309.
[25] S.-E. Park, J.-S. Chang, J.S. Yoo, in: M.M. Maroto-Valer, Y. Soong, C. Song (Eds.), Environmental Challenges and Greenhouse Gas Control for Fossil Fuel Utilization in 21 Century, Kluwer Academic Publishers/Plenum Press, New York, 2001, pp. 359–369.
[26] V.P. Vislovskiy, J.-S. Chang, M.-S. Park, S.-E. Park, Catal. Commun. 3 (2002) 227.
[27] B. Grzybowska-Swierkosz, F. Trifirò, J.C. Vedrine (Eds.), Appl. Catal. A 157 (1997) (special issue).
[28] E.A. Mamedov, V. Cortes Corberan, Appl. Catal. A 127 (1995) 1 (review).
[29] R.G. Rizayev, E.A. Mamedov, V.P. Vislovskii, V.E. Sheinin, Appl. Catal. A 83 (1992) 103 (review).
[30] V.P. Vislovskiy, V.Yu. Bychkov, M.Yu. Sinev, N.T. Shamilov, P. Ruiz, Z. Schay, Catal. Today 61 (2000) 325.
[31] M. Bañares, I.E. Wachs (Eds.), Catal. Today 78 (2003) (special issue).
[32] I.P. Belomestnykh, E.A. Skrigan, N.N. Rozhdestvenskaya, G.V. Isaguliants, Stud. Surf. Sci. Catal. 72 (1992) 453.
[33] J. Hanuza, B. Jezowska-Trzebiatowska, W. Oganowski, J. Mol. Catal. 29 (1985) 109.
[34] W.S. Chang, Y.Z. Chen, B.L. Yang, Appl. Catal. A 124 (1995) 221.
[35] E.A. Mamedov, R.M. Talyshinskii, R.G. Rizayev, J.L.G. Fierro, V. Cortes Corberan, Corberan. Catal. Today 32 (1996) 177.

[36] J.F. Moulder, et al., Handbook of X-ray Photoelectron Spectroscopy, Perkin-Elmer Corp.
[37] J. Mendiadua, R. Casanova, Y. Barbaux, J. Electr. Spectr. Relat. Phenom. 71 (1995) 249.
[38] M. Coranne, J. Goodwin, G. Marcelin, J. Catal. 148 (1994) 388.
[39] W.S. Chang, Y.Z. Chen, B.L. Yang, Appl. Catal. A 124 (1995) 221.
[40] G. Bosch, B.J. Kip, J.G. Van Ommen, P.J. Gellings, J. Chem. Soc., Faraday Trans. I 80 (1984) 2479.
[41] M.A. Volpe, Appl. Catal. A 210 (2001) 355.
[42] V.P. Vislovskiy, N.T. Shamilov, V.Yu. Bychkov, M.Yu. Sinev, P. Ruiz, V. Cortes Corberan, in preparation.
[43] I.E. Wachs, B.M. Weckhuysen, Appl. Catal. A 157 (1997) 67.
[44] J. Haber, in: G. Ertl, H. Knözinger, J. Weitkamp (Eds.), Handbook of Heterogeneous Catalysis, vol. 5, VCH, Weinheim, 1997, p. 2253.
[45] B. Grzybowska-Swierkosz, Appl. Catal. A 157 (1997) 409.
[46] T.M. Blasco, J.M. Lopez Nieto, Appl. Catal. A 157 (1997) 117.
[47] V.Yu. Bychkov, M.Yu. Sinev, V.P. Vislovskii, Kinet. Catal. (Eng. Trans.) 42 (2001) 574.
[48] E.M. Gaigneaux, H.M. Abdel Dayem, E. Godard, P. Ruiz, Appl. Catal. A 202 (2000) 265.
[49] J. Le Bars, A. Auroux, M. Forissier, J.C. Vedrine, J. Catal. 162 (1996) 250.
[50] G. Centi, F. Marchi, S. Perathoner, Appl. Catal. A 149 (1997) 225.
[51] G. Centi, S. Perathoner, F. Trifirò, Appl. Catal. A 157 (1997) 143.
[52] J. Datka, Z. Sarbak, R.P. Eischens, J. Catal. 145 (1994) 544.
[53] B. Delmon, Surf. Rev. Lett. 2 (1995) 25.
[54] L.T. Weng, P. Ruiz, B. Delmon, Stud. Surf. Sci. Catal. 72 (1992) 399.
[55] C. Li, Q. Xin, P. Ruiz, X.X. Guo, B. Delmon, J. Mol. Catal. 72 (1992) 307.
[56] F. Dury, E.M. Gaigneaux, P. Ruiz, Appl. Catal. A 242 (2003) 187.